

# Application of the Surface Area Approach to the Correlation and Estimation of Aqueous Solubility and Vapor Pressure. Alkyl Aromatic Hydrocarbons

Gordon L. Amidon\* and Shabir T. Anik†

School of Pharmacy, University of Wisconsin, Madison, Wisconsin 53706

A group surface area approach is developed and applied to the estimation of the free energy changes for the following processes: (I) pure (supercooled) liquid to aqueous solution ( $\Delta G_1^\circ$ ), (II) pure (supercooled) liquid to gas ( $\Delta G_2^\circ$ ), and (III) gas to aqueous solution ( $\Delta G_3^\circ$ ). The corresponding estimates of solubility (pure liquid/solution and gas/solution) and vapor pressure at 298 K are easily made. The standard error of the estimate in the worst case (gas to solution) is only 1.1 kJ mol<sup>-1</sup>. Analysis of the surface area models shows that the single variable total surface area, TSA, can be used to estimate the pure (supercooled) liquid to aqueous solution free energy change,  $\Delta G_1^\circ$ , with a standard error of 1.1 kJ/mol. This apparent simplicity is due to compensating changes in  $\Delta G_2^\circ$  and  $\Delta G_3^\circ$ . For the latter two steps a partitioning of the TSA into group areas is required. Within the context of the surface area model, this is attributed to significant differences in surface area coefficients for the aliphatic and aromatic hydrogens. The particular choice of group surface area terms in the final selected model shows good additivity as measured by application of the method to compounds not included in the study.

## Introduction

The estimation of physical properties using correlating parameters usually involves an inherent compromise between accuracy and ease of calculation. In previous work it has been shown that molecular and group surface areas can be employed in an efficient and relatively reliable manner to compute aqueous solubilities (1-3). In a more recent study the three steps in the thermodynamic cycle

pure (supercooled) liquid  $\rightarrow$  gas

gas  $\rightarrow$  aqueous solution

pure (supercooled) liquid  $\rightarrow$  aqueous solution

were analyzed for polycyclic aromatic compounds with excellent results (4). However, it was clearly noted that there were significant differences between aliphatic and polycyclic aromatic compounds for the various cycle steps. In this report we have investigated the application of the surface area approach to alkyl aromatic compounds. The objectives of this study were (i) to assess the utility of the surface area approach in estimating both aqueous solubility (pure liquid to water and gas phase to water) and vapor pressures of alkyl aromatic compounds, (ii) to develop the simplest surface area model consistent with reasonable accuracy, and (iii) to assess the additivity (or nonadditivity) of the model of alkyl aromatic compounds.

## Experimental Section

**Materials.** 1,4-Dimethylnaphthalene (99%), 2,3-dimethylnaphthalene (99%), 2,6-dimethylnaphthalene (99%), and 9,10-dimethylantracene (99%) were obtained from Aldrich Chemical Co. and were used without further purification. Ethanol (95%, Commercial Solvents Inc.) was distilled before use. All water used was double distilled with final distillation from alkaline permanganate.

**Solubility Determinations. 9,10-Dimethylantracene.** The solid was equilibrated in 15-mL ampules containing from 8 to 10 mL of water by end-on-end rotation in a water bath maintained at 25 °C. The water in the ampule was deaerated by a stream of nitrogen before sealing. The solutions were sampled at different periods of time to check whether equilibration was complete. Eighteen days were required to achieve equilibrium. The number of days may be a function of the container and the method of equilibration. Samples were obtained by filtration through a glass-wool plug on a pipet tip and were assayed by fluorimetric analysis.

**1,4-Dimethylnaphthalene.** This is a liquid of density  $\sim 1$  g/cm<sup>3</sup>. Following equilibration the ampules were centrifuged at 6000 rpm for 10 min in a temperature-controlled Beckman centrifuge. Ten minutes was sufficient time to separate the two phases although a fine film still remained at the surface. After centrifugation 5 mL of solution was withdrawn from the center of the ampule by means of a syringe, taking care not to touch the sides or the bottom of the ampule. The 5 mL was immediately diluted to 10 mL by rinsing the syringe with 95% ethanol into a volumetric flask. The solution was then assayed by measuring the absorbance at 288.5 nm. The sample reached a constant value after 10 days of equilibration as described above.

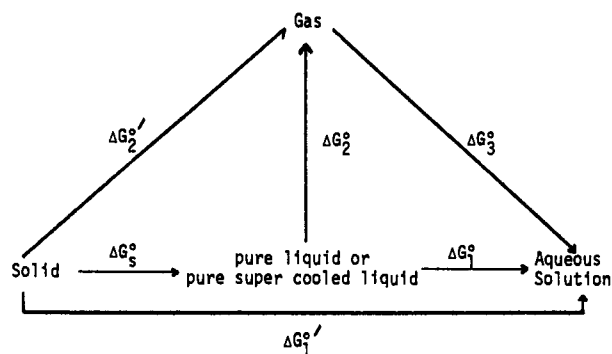
**Spectral Methods. UV.** 2,3-Dimethylnaphthalene, 2,6-dimethylnaphthalene, and 1,4-dimethylnaphthalene were measured by UV absorption on the Cary 16 spectrophotometer. Standard solutions were prepared in 95% ethanol. Linear graphs were obtained, giving molar absorptivities of  $4.968 \times 10^3$  ( $\lambda_{\text{max}} = 278$  nm),  $4.677 \times 10^3$  ( $\lambda_{\text{max}} = 273$  nm), and  $6.839 \times 10^3$  ( $\lambda_{\text{max}} = 288.5$  nm), respectively. In the case of 1,4-dimethylnaphthalene a standard curve for solutions in 47.5% ethanol was also prepared for use in the solubility measurement and gave a molar absorptivity of  $6.532 \times 10^3$  ( $\lambda_{\text{max}} = 288.5$ ).

**Fluorimetry.** 9,10-Dimethylantracene was assayed by fluorimetric analysis on a Perkin-Elmer MP-4 spectrofluorimeter. The difficulty that arises is the preparation of the standard curve for aqueous solutions. However Schwarz (8) has shown that the quantum yield of these polycyclic aromatics is about the same in both water and ethanol provided the solutions are purged with nitrogen to remove all dissolved oxygen before taking the reading. Hence a standard curve was prepared by using 95% ethanol solutions of dimethylantracene. The  $\lambda_{\text{ex}}$  is 259 nm and  $\lambda_{\text{em}}$  = 402 nm. A linear graph was obtained for fluorescence peak height vs. concentration.

**Vapor Pressures and Heats of Fusion.** Vapor pressures and heats of fusion (for solids) were determined as previously reported (4) and are given in Appendix A (see paragraph at end

† Present address: Institute of Pharmaceutical Sciences, Syntex Research, Palo Alto, CA 94304

Scheme I



of text regarding supplementary material).

### Method

Additivity in physical property estimation is best achieved on a free energy basis. Scheme I presents the thermodynamic cycle used for the free energy calculations

$$\Delta G_1^\circ = -RT \ln x_s \quad (1)$$

$$\Delta G_2^\circ = -RT \ln p^\circ \quad (2)$$

$$\Delta G_3^\circ = -RT \ln (x_s/p^\circ) = RT \ln k \quad (3)$$

where  $x_s$  is the mole fraction aqueous solute solubility,  $p^\circ$  the pure liquid (or cooled liquid) solute vapor pressure (in atmospheres), and  $k$  the Henry's law constant.

For compounds that are solids at room temperature, the correction to the supercooled liquid must be made (2) as follows (Scheme I): for the pure supercooled liquid to gas step

$$\Delta G_2^\circ = \Delta G_2^{\circ'} - \Delta G_s^\circ \quad (4)$$

for the pure supercooled liquid to aqueous solution step

$$\Delta G_1^\circ = \Delta G_1^{\circ'} - \Delta G_s^\circ \quad (5)$$

where

$$\Delta G_s^\circ = \Delta H_f^\circ(T_m - T)T_m \quad (6)$$

$\Delta G_2^{\circ'}$  and  $\Delta G_1^{\circ'}$  refer to the solid-to-gas and solid-to-solution steps, respectively,  $\Delta H_f^\circ$  is the heat of fusion at the melting point,  $T_m$ , and  $T$  is the temperature of interest, 298 K.  $\Delta G_s^\circ$  is a measure of the lattice energy of the solid (crystal), and the importance of its consideration in solute-solvent interactions may be illustrated by the following examples. (i) In a study of the effect of chain length on the solubility for a homologous series of compounds, the higher homologues may be solids. The change in solubility of the solid homologue may be a result of the additional lattice energy of the crystal rather than any dramatic change in its behavior toward the solvent. Correction for this lattice energy by  $\Delta G_s^\circ$  then allows comparison of the lower liquid homologues with the higher solid homologues (5). (ii) Anthracene and phenanthrene are isomers but have aqueous solubilities differing by a factor of 100. Their activity coefficients in water however are very similar (6). The difference in solubility is almost entirely due to the difference in their solid-state interactions and can be accounted for by the above correction (4). The aqueous solubilities, heats of fusion, and vapor-pressure data used for this analysis are presented in Appendix A (supplementary material). For vapor pressures not reported, the free energy values,  $\Delta G_2^\circ$  were taken directly from ref 7.

From previous results of the analysis of aqueous solubilities using the molecular surface area approach (2, 3), the free

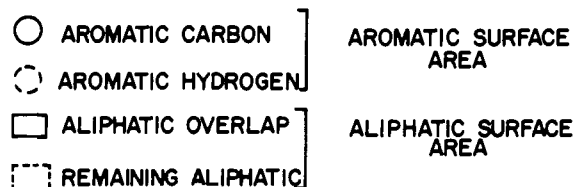
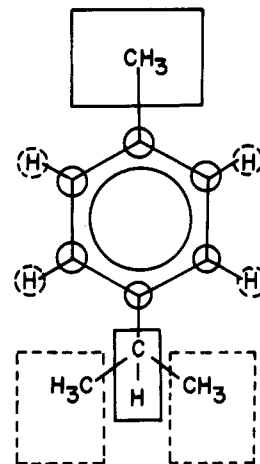


Figure 1. Partitioning of total surface area into group areas: ArC = aromatic carbon; ArH = aromatic hydrogen; AlOv = aliphatic overlap; and ReAL = remaining aliphatic.

energy change may be related to the surface area group contributions by the general equation:

$$\Delta G^\circ = \theta_0 + \sum_{i=1}^n \theta_i(\text{GSA})_i \quad (7)$$

where the  $\theta_i$  values are parameters with units of  $\text{J}/(\text{mol } \text{\AA}^2)$ , and  $(\text{GSA})_i$  is the surface area of the  $i$ th kind of group of atoms. Group additivity in eq 7 is strongly dependent on atom grouping. For the alkyl aromatics, the total surface area may be partitioned into an aromatic surface area, which is the sum of the surface areas of the aromatic carbons and hydrogens, and an aliphatic surface area, which may be divided into an aliphatic overlap and a remaining aliphatic area. The overlap area is defined as the area of the aliphatic carbon atom with its attached hydrogens which is adjacent to the aromatic nucleus (4). The different groups of atomic surface areas are shown in Figure 1.

The parameters of eq 7 were determined by regression analysis. The data set consisted of 5 alkanes, 14 alkyl-benzenes, and 5 polycyclic aromatics. All surface areas were calculated by the method of Hermann (7) using a 1.5- $\text{\AA}$  solvent radius. Table I lists the free energy data and the surface area contributions for all the compounds used in the regression analysis.

### Results and Discussion

The first step in the analysis of the solution properties of the alkyl aromatics is to compare the results with the aliphatic and aromatic hydrocarbons. Figures 2 and 3 present the free energy change with total surface area (TSA) of these three classes of compounds for the pure liquid to aqueous solution and gas to aqueous solution processes. Several observations may be noted: (i) the free energy change for the pure liquid to aqueous solution (Figure 2) process ( $\Delta G_1^\circ$ ) shows good correlation with the TSA of the molecule for all three classes of compounds, and the alkyl aromatic and polycyclic aromatic compounds lie on essentially the same straight line with a slope similar to that of the alkanes; (ii) the correlation between the free energy change and TSA for the alkyl aromatics is much

Table I. Free Energy (kJ/Mol) and Surface Area ( $\text{\AA}^2$ ) Contributions for the Compounds Used in the Regression Analysis<sup>a, b</sup>

| compd                       | ArC   | ArH   | ArSA  | AIOV  | ReAL  | AISA  | TSA   | $\Delta G_1^\circ$ | $\Delta G_2^\circ$ | $\Delta G_3^\circ$ |
|-----------------------------|-------|-------|-------|-------|-------|-------|-------|--------------------|--------------------|--------------------|
| benzene                     | 85.6  | 170.1 | 255.7 | 0.0   | 0.0   | 0.0   | 255.7 | 19.4               | 5.16               | 14.2               |
| toluene                     | 72.7  | 129.8 | 202.5 | 84.0  | 0.0   | 84.0  | 286.5 | 22.7               | 8.25               | 14.4               |
| ethylbenzene                | 65.5  | 125.5 | 190.9 | 44.0  | 80.3  | 124.7 | 315.6 | 26.1               | 10.9               | 15.2               |
| <i>o</i> -xylene            | 62.9  | 101.8 | 164.7 | 145.0 | 0.0   | 145.0 | 309.7 | 25.9               | 11.6               | 14.3               |
| <i>m</i> -xylene            | 59.4  | 90.2  | 149.6 | 168.0 | 0.0   | 168.0 | 317.6 | 26.0               | 11.2               | 14.8               |
| <i>p</i> -xylene            | 59.4  | 90.2  | 149.6 | 168.0 | 0.0   | 168.0 | 317.6 | 25.7               | 11.2               | 14.6               |
| propylbenzene               | 65.4  | 125.5 | 190.9 | 33.4  | 123.1 | 156.5 | 347.4 | 29.0               | 12.6               | 16.5               |
| isopropylbenzene            | 60.0  | 119.4 | 179.4 | 6.9   | 152.0 | 159.0 | 338.4 | 28.7               | 12.7               | 15.9               |
| 1,2,3-trimethylbenzene      | 53.4  | 73.4  | 126.8 | 205.6 | 0.0   | 205.6 | 332.4 | 28.3               | 14.2               | 14.0               |
| 1,2,4-trimethylbenzene      | 49.8  | 61.8  | 111.6 | 229.0 | 0.0   | 229.0 | 340.6 | 29.0               | 14.4               | 14.6               |
| 1,3,5-trimethylbenzene      | 46.3  | 50.2  | 96.5  | 252.1 | 0.0   | 252.1 | 348.6 | 28.3               | 14.1               | 14.2               |
| butylbenzene                | 65.4  | 125.5 | 190.9 | 33.4  | 155.0 | 188.4 | 379.3 | 33.0               | 14.9               | 18.1               |
| <i>sec</i> -butylbenzene    | 59.4  | 123.0 | 182.4 | 2.0   | 183.0 | 185.0 | 367.4 | 31.3               | 15.0               | 16.3               |
| <i>tert</i> -butylbenzene   | 57.3  | 110.4 | 167.7 | 0.0   | 185.0 | 185.0 | 352.7 | 30.6               | 14.6               | 16.1               |
| 1-methyl-4-isopropylbenzene | 46.9  | 79.4  | 126.3 | 100.0 | 143.0 | 243.0 | 369.3 | 30.5               | 15.4               | 15.1               |
| naphthalene                 | 120.2 | 203.1 | 323.3 | 0.0   | 0.0   | 0.0   | 323.3 | 27.4               | 19.6               | 7.83               |
| anthracene                  | 154.9 | 236.0 | 390.9 | 0.0   | 0.0   | 0.0   | 390.9 | 34.9               | 36.1               | -1.21              |
| phenanthrene                | 155.1 | 229.2 | 384.3 | 0.0   | 0.0   | 0.0   | 384.3 | 35.6               | 34.1               | 1.51               |
| pyrene                      | 165.5 | 236.0 | 401.5 | 0.0   | 0.0   | 0.0   | 401.5 | 40.0               | 41.4               | -1.38              |
| butane                      | 0.0   | 0.0   | 0.0   | 0.0   | 255.0 | 255.0 | 255.0 | 24.7               | -2.18              | 26.9               |
| pentane                     | 0.0   | 0.0   | 0.0   | 0.0   | 287.0 | 287.0 | 287.0 | 28.5               | 1.09               | 27.4               |
| hexane                      | 0.0   | 0.0   | 0.0   | 0.0   | 319.0 | 319.0 | 319.0 | 32.7               | 4.10               | 28.5               |
| heptane                     | 0.0   | 0.0   | 0.0   | 0.0   | 351.0 | 351.0 | 351.0 | 36.0               | 6.99               | 29.0               |
| octane                      | 0.0   | 0.0   | 0.0   | 0.0   | 383.0 | 383.0 | 383.0 | 39.8               | 9.92               | 29.8               |

<sup>a</sup> Surface areas calculated by using a 1.5- $\text{\AA}$  solvent radius. <sup>b</sup> For solids, the free energy changes refer to the supercooled liquid.<sup>7</sup>

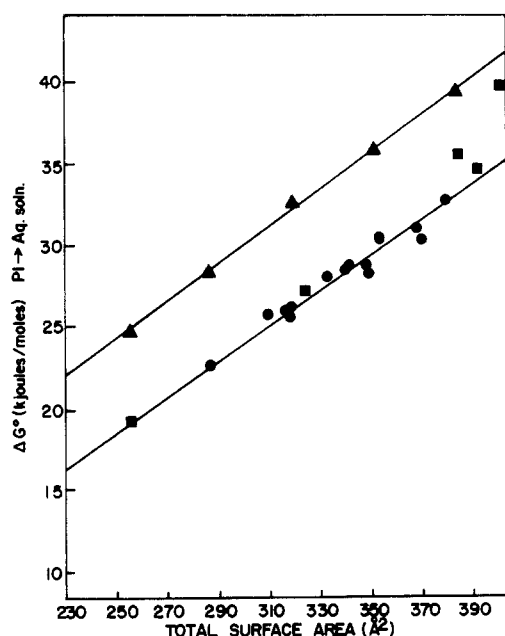


Figure 2. Free energy of solution vs. total surface area for aliphatic ( $\blacktriangle$ ), aromatic ( $\blacksquare$ ), and alkyl aromatic ( $\bullet$ ) hydrocarbons.

poorer for the gas-to-solution process ( $\Delta G_3^\circ$ ), Figure 3, and furthermore the aromatic and alkyl aromatic compounds do not lie on the same line; (iii) this suggests that the linearity observed for  $\Delta G_1^\circ$  is a result of considerable free energy compensation; and (iv) as one might expect, the slopes of the lines for the *n*-alkylbenzenes are similar to those for the *n*-alkanes, indicating the independence of the  $\text{CH}_2$  group at greater distances from the aromatic nucleus.

Perhaps the most striking observation, however, is that the "hydrophobic" nature of the methyl groups attached to the aromatic nucleus is quite different from that commonly observed for methyl groups (4). From Figure 3 and Table I it can be noted that all of the polymethylbenzenes fall below the line for the *n*-alkylbenzenes (the line for the alkyl aromatic compounds in Figure 3 is drawn through the *n*-alkyl derivatives only). Furthermore, in going from benzene to toluene, there is an

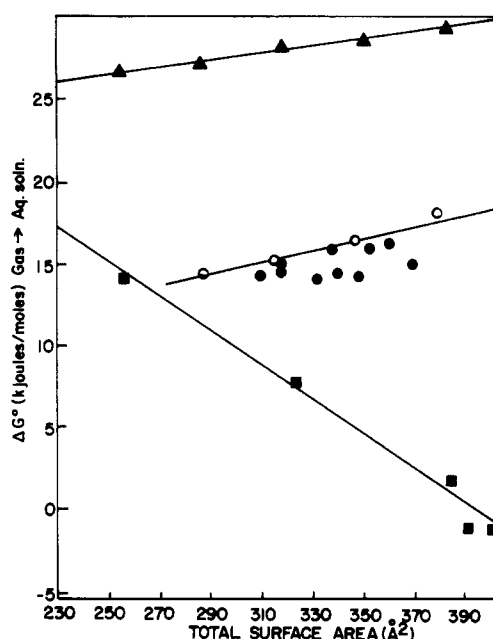


Figure 3. Free energy of hydration (step 3, Scheme I) vs. total surface area for aliphatic ( $\blacktriangle$ ), aromatic ( $\blacksquare$ ), *n*-alkyl aromatic ( $\circ$ ), and alkyl aromatic ( $\bullet$ ) hydrocarbons.

increase of only 209 J/mol in the free energy of solvation,  $\Delta G_3^\circ$ , while the surface area increases by 31  $\text{\AA}^2$ . As another example, the surface area of 1,2,3-trimethylbenzene is 77  $\text{\AA}^2$  larger than benzene, yet the solvation free energies are nearly the same. If the methyl group contribution (e.g., replacement of an aromatic hydrogen with a  $\text{CH}_3$  group) were similar to that for aliphatic compounds, the expected free energy increase would be  $\sim 780$  and 1900 J/mol, respectively (10). Although there is considerable variation in the data (Appendix A), the significance of this result is reinforced by the fact that the  $\Delta G_3^\circ$  values for all of the polymethylbenzenes are similar to that for benzene (Table I) despite significantly larger surface areas.

These results indicate that replacement of an aromatic hydrogen by the much larger methyl group has little net effect on the free energy of solvation ( $\Delta G_3^\circ$ ). Consequently the aromatic

Table II. Results of Regression Analysis for the Model  $\Delta G^\circ = \Theta_0 + \Theta_1 \text{ArC} + \Theta_2 \text{ArH} + \Theta_3 \text{AIOV} + \Theta_4 \text{ReAL} + \Theta_5 I^a$ 

| process    | $\Theta_0$     | $\Theta_1$       | $\Theta_2$       | $\Theta_3$      | $\Theta_4$       | $\Theta_5$     | $r$   | $s$  |
|------------|----------------|------------------|------------------|-----------------|------------------|----------------|-------|------|
| pl → soln  | -2.47<br>(1.9) | 0.193<br>(0.04)  | 0.059<br>(0.04)  | 0.100<br>(0.01) | 0.109<br>(0.004) | -4.94<br>(2.1) | 0.991 | 0.75 |
| pl → gas   | -25.5<br>(2.2) | 0.557<br>(0.04)  | -0.134<br>(0.05) | 0.063<br>(0.02) | 0.092<br>(0.008) | 6.09<br>(2.47) | 0.997 | 0.88 |
| gas → soln | 23.0<br>(2.5)  | -0.360<br>(0.05) | 0.193<br>(0.05)  | 0.038<br>(0.02) | 0.017<br>(0.008) | 11.0<br>(2.85) | 0.994 | 1.1  |

<sup>a</sup> Values in parentheses are standard errors;  $r$  = correlation coefficient;  $s$  = standard error of regression; no. of data points = 24.  $\Delta G^\circ$  in units of kJ/mol.

hydrogens and methyl groups adjacent to the aromatic ring must be treated as distinct units in any general model.

#### Model for Estimating the Free Energy Changes for the Cycle Steps for the Alkyl Aromatics

The simplest model other than using the total surface area is to partition it into aromatic (ArSA) and aliphatic (AISA) contributions and can be written as

model 1

$$\Delta G = \Theta_0 + \Theta_1 \text{ArSA} + \Theta_2 \text{AISA} + \Theta_3 I$$

This however relies on the additivity of the separate contributions of the alkyl and aromatic portions and, on the basis of the above considerations, will not be a satisfactory model for cycle steps 2 and 3. Given the data for the polymethyl aromatic compounds, any model must include a term or terms to account for the different nature of the methyl or methylene group adjacent to the aromatic nucleus. The terms in model 1 can be partitioned further to give the following hierarchy of models:

model 2

$$\Delta G = \Theta_0 + \Theta_1 \text{ArSA} + \Theta_2 \text{AIOV} + \Theta_3 \text{ReAL} + \Theta_4 I$$

model 3

$$\Delta G = \Theta_0 + \Theta_1 \text{ArC} + \Theta_2 \text{ArH} + \Theta_3 \text{AISA} + \Theta_4 I$$

model 4

$$\Delta G = \Theta_0 + \Theta_1 \text{ArC} + \Theta_2 \text{ArH} + \Theta_3 \text{AIOV} + \Theta_4 \text{ReAL} + \Theta_5 I$$

The various group areas are defined as in Figure 1. In each case the group areas add up to the total surface of the molecule.  $I$  is an indicator variable and accounts for the presence of an aromatic group. It has the value of 1 for the alkyl and polycyclic aromatics and 0 for the alkanes and is similar to the IFG coefficient discussed in earlier work (3). Several other models were also tested incorporating dipole moments, polarizabilities, and various definitions for the overlap area such as the sum of alkyl and attached aromatic carbon and two carbon contributions of the alkyl chain. These additional terms did not significantly improve the correlation ( $\beta$ ). The alkanes and the polycyclic aromatics were included in the data set for two reasons: (i) we wanted to uncouple correlations between some of the group surface area terms, and (ii) the polycyclic aromatics give a wider range of values for the free energy changes and hence allow extension of the model to alkyl derivatives of the higher aromatics such as the alkylnaphthalenes, anthracenes, and polycyclic aromatics. Of the several models studied, model 4 is the most satisfactory model for  $\Delta G_2^\circ$  and  $\Delta G_3^\circ$ , while all of the models work well for  $\Delta G_1^\circ$  ( $\beta$ ). The regression results for model 4 are presented in Table II.

**Pure-Liquid Solubility.** Comparing the results for  $\Delta G_1^\circ$  by using model 4 (Table II) with model 1

$$\Delta G_1^\circ = -4.72 + 0.126 \text{ArSA} + 0.117 \text{AISA} - 7.61 I$$

(1.51)      (0.004)      (0.004)      (0.59)

where  $n = 24$ ,  $r = 0.99$ , and  $s = 0.80$ , shows them to have

similar overall statistics. Furthermore, the similarity of the ArSA and AISA coefficients in model 1 suggests a further reduced model

$$\Delta G_1^\circ = -6.47 + 0.122 \text{TSA} - 5.94 I$$

(1.95)      (0.006)      (0.57)

where  $n = 24$ ,  $r = 0.98$ , and  $s = 1.1$ . Equation 8 is surprisingly good given its simplicity. Only one variable, TSA, ( $I$  is a classification variable) is needed to estimate the pure liquid (or supercooled liquid) to aqueous solution free energy change with a standard error of 1.1 kJ/mol. Furthermore, the TSA variable can be roughly estimated itself by using correlations taken from Table I. Hence eq 8 can easily be used to qualitatively estimate  $\Delta G_1^\circ$  for aliphatic, aromatic, and alkyl aromatic compounds.

For estimating liquid (supercooled liquid) solubility at 298 K, the equation

$$-\log x_s = \Delta G_1^\circ / (2.303 RT) = (1.75 \times 10^{-4}) \Delta G_1^\circ$$

is used. It should be noted that for solids the  $\Delta G_s^\circ$  contribution must be included (eq 6). That is

$$-\log x_s = \Delta G_1^{\circ'} / (2.303 RT) = (\Delta G_s^\circ + \Delta G_1^\circ) / (2.303 RT)$$

The success of model 1 and eq 8 for  $\Delta G_1^\circ$  is due to compensating changes in  $\Delta G_2^\circ$  and  $\Delta G_3^\circ$  since, as shown below, model 1 is not nearly as successful as model 4 for  $\Delta G_2^\circ$  and  $\Delta G_3^\circ$ .

**Gas-Phase Solubility.** The free energy change for the gas phase to solution step,  $\Delta G_3^\circ$ , in Table II is calculated from eq 3. The implied assumption is that Henry's law applies up to the aqueous solubility (4). Hence the aqueous concentration (solubility) at any pressure,  $P$ , below  $P^\circ$  is given by

$$x = P/k$$

with  $k$  being estimated from  $\Delta G_3^\circ$ .

For this step, model 4 is superior to model 1 ( $r = 0.994$  compared with  $r = 0.958$ , ref 8). If one assumes that the magnitudes of the coefficients reflect the free energy of interaction ( $\delta \Delta G^\circ / \text{\AA}^2$ ) of a particular group with water, the coefficients of model 4 suggest the following: (i) the aromatic carbons are intrinsically hydrophilic and (ii) the aromatic hydrogens are more intrinsically hydrophobic than the aliphatic hydrogens. Although the ArC and ArH terms are highly correlated ( $r = 0.975$ ), the standard errors of the coefficients are not excessively large and both coefficients are significant at the 95% confidence level. This interpretation is consistent with the observed data where replacement of an aromatic hydrogen by a methyl group has less of an effect on  $\Delta G_3^\circ$  than expected (see above).

A comparison of benzene and toluene illustrates the above points. The changes in the surface area terms, (toluene) - (benzene), are -12.9, -40.3, and 84  $\text{\AA}^2$  for the ArC, ArH, and AIOV terms, respectively. The corresponding contributions to the  $\delta \Delta G_3^\circ$  (toluene - benzene) are 4.64, -7.77, 3.17 kJ/mol, with a resulting  $\delta \Delta G_3^\circ(\text{est}) = 0.062$  kJ/mol and  $\delta \Delta G_3^\circ(\text{exptl}) = 0.2$  kJ/mol. Thus the positive contributions resulting from a reduction in ArC and an increase in AIOV are offset by a large

Table III. Group Surface Areas and Observed and Predicted Values of the Free Energy of Hydration for the Alkyl-naphthalenes

| compd                   | ArC    | ArH   | AIOV  | ReAL | TSA   | $\Delta G_3^\circ$ , kJ/mol |      |
|-------------------------|--------|-------|-------|------|-------|-----------------------------|------|
|                         |        |       |       |      |       | obsd                        | pred |
| naphthalene             | 120.2  | 203.1 | 0.0   | 0.0  | 232.3 | 7.83                        | 7.74 |
| 1-methylnaphthalene     | 180.0  | 164.6 | 74.0  | 0.0  | 347.4 | 7.03                        | 7.70 |
| 2-methylnaphthalene     | 107.4  | 162.7 | 84.1  | 0.0  | 354.1 | 8.25                        | 7.88 |
| 2,3-dimethylnaphthalene | 97.5   | 134.4 | 145.8 | 0.0  | 377.6 | 8.12                        | 8.33 |
| 2,6-dimethylnaphthalene | 94.6   | 122.4 | 168.0 | 0.0  | 385.0 | 9.67                        | 7.87 |
| 1,4-dimethylnaphthalene | 95.7   | 126.1 | 149.0 | 0.0  | 370.8 | 6.40                        | 7.49 |
| 1-ethylnaphthalene      | 103.6  | 154.0 | 38.5  | 76.5 | 373.6 | 7.45                        | 7.16 |
| 2-ethylnaphthalene      | 100.00 | 158.4 | 44.3  | 80.4 | 383.1 | 8.58                        | 9.54 |

Table IV. Surface Areas ( $\text{\AA}^2$ ) and Observed and Predicted Free Energies (kJ/Mol) of Solution for Some Polycyclic Aromatics<sup>a</sup>

| compd                    | ArC   | ArH   | AIOV  | ReAL | TSA   | $\Delta G_1^\circ$ |                   |
|--------------------------|-------|-------|-------|------|-------|--------------------|-------------------|
|                          |       |       |       |      |       | obsd               | pred <sup>c</sup> |
| 9,10-dimethylanthracene  | 132.0 | 165.0 | 128.0 | 0.0  | 425   | 41.6               | 40.52             |
| chrysene                 | 190.1 | 255.3 | 0.0   | 0.0  | 445.4 | 43.4               | 44.1              |
| 1,2:5,6-dibenzanthracene | 224.7 | 288.3 | 0.0   | 0.0  | 513.0 | 45.8 <sup>b</sup>  | 52.8              |
| 1,2-benzopyrene          | 237.0 | 234.2 | 0.0   | 0.0  | 471.1 | 48.8               | 46.5              |
| 1,2-benzanthracene       | 189.8 | 262.1 | 0.0   | 0.0  | 451.9 | 44.5               | 44.5              |
| perylene                 | 200.6 | 255.4 | 0.0   | 0.0  | 456.0 | 45.7               | 46.2              |

<sup>a</sup> Experimental data in Appendix A. <sup>b</sup> The observed solubility appears to be rather high. <sup>c</sup> Predicted solubilities calculated by using model 4.

negative contribution from a reduced ArH term.

The above interpretation is based entirely on surface area correlations. One of the limitations of this approach is that it does not directly account for the influence of substituents on the electronic changes in the molecule. This might be particularly relevant for the alkylbenzenes where increasing methyl substitution increases the Lewis basicity or hydrogen bonding ability of the aromatic nucleus (9). The correlation coefficient between the ArH area and the corresponding Lewis basicity is  $-0.86$ , indicating that the ArH area reflects to some extent the Lewis basicity and the improvement in the statistics of the model with the inclusion of the ArH term may in part be due to this correlation. Hence the favorable  $\delta\Delta G^\circ$  of solvation with increasing methyl substitution could also be explained as being a result of changes in the  $\Pi$  character of the aromatic nucleus. The surface area method however cannot differentiate between these two alternatives but has the advantage of not requiring experimental data in order to account for the effect.

**Vapor Pressure.** For the pure liquid to gas phase process, model 4 is again the most appropriate. Model 1 is much less satisfactory with a standard error of 2.9 kJ/mol. The vapor pressure of the pure (supercooled) liquid is calculated from eq 2.

As in the previous discussion of the contributing cycle steps, the relative magnitudes of the coefficients may be interpreted in terms of the contribution of the different group surface areas to the free energy of vaporization. The positive coefficient for the aromatic carbon area may be attributed to the strong interaction between the aromatic residues in the pure liquid phase. The ArH coefficient is negative and suggests a decrease in the free energy of vaporization with increasing ArH area, while the AIOV and ReAL coefficients are positive and result in increasing free energies of vaporization with increasing group surface area. The coefficient of the ReAL term is identical with that for the alkanes and suggests an independence of the methylene and aromatic group at longer chain lengths. A consequence of the different contributions of the group surface areas is the correct prediction that the polymethylbenzenes have a higher free energy of vaporization (lower vapor pressure) compared to corresponding *n*-alkylbenzene. Finally it may be noted that the major portion of the change in the free energy of solution ( $\Delta G_1^\circ$ ) with increasing methyl substitution is largely a result of the increased interaction of the polymethylbenzenes in the pure liquid phase (10).

**Model Predictions.** The value of the above analysis is further enhanced by its extension to estimating the solution properties of compounds which were not included in the original analysis. Table III lists surface area contributions and observed and predicted free energies of hydration,  $\Delta G_3^\circ$ , for naphthalene and some of its alkyl derivatives, where the predicted free energies were calculated by using model 4. In most cases the model is qualitatively correct in predicting the effects of the methyl group on the gas-phase solubility. The standard error of the prediction is 0.89, which is somewhat smaller than the standard error in Table III (1.1), indicating no lack of fit. Thus in going from 1- to 2-methylnaphthalene, the solubility decreases, whereas, in going from 2,3-dimethylnaphthalene to 1,4-dimethylnaphthalene, the solubility increases as estimated. The agreement between observed and estimated values for  $\Delta G_1^\circ$  and  $\Delta G_2^\circ$  is also good.

Table IV contains compounds for which only data for  $\Delta G_1^\circ$  are available. Except for 1,2:5,6-dibenzanthracene, the agreement is very good. Thus, the surface area approach, combined with the group area definitions employed, appears to be able to provide useful estimates of the solution free energy changes. A potential application of this approach is to vary insoluble hydrocarbon compounds for which accurate experimental data are unavailable or difficult to obtain.

## Summary

The group surface area approach has been shown to give excellent estimates of the free energy changes associated with the following three processes (see Scheme I): (i) pure (supercooled) liquid to aqueous solution ( $\Delta G_1^\circ$ ), (ii) pure (supercooled) liquid to gas ( $\Delta G_2^\circ$ ), and (iii) gas to aqueous solution ( $\Delta G_3^\circ$ ). The most satisfactory model is

$$\Delta G^\circ = \theta_0 + \theta_1 \text{ArC} + \theta_2 \text{ArH} + \theta_3 \text{AIOV} + \theta_4 \text{ReAL} + \theta_5 I$$

where the coefficients for each equilibrium step are given in Table II and the surface area terms defined in Figure 1. The standard error of the estimate in the worst case (gas to solution) is only 1.1 kJ/mol (0.26 kcal/mol). The surface area partitioning scheme in Figure 1 combined relative simplicity with a high degree of additivity. The additivity was tested through calculations on compounds not included in the regression analysis, alkyl-naphthalenes and polycyclic aromatics. In both cases agreement was excellent, with the standard error of the pre-

diction not significantly different from that for compounds used in the original regression analysis.

For the pure (supercooled) liquid to aqueous solution step, a very simple model involving the total surface area (TSA) of the molecule can be used to estimate  $\Delta G_1^\circ$  for alkyl, aromatic, and alkyl aromatic hydrocarbons. The apparent success of this simple model for  $\Delta G_1^\circ$  is due to considerable free energy compensation since it is much less satisfactory for  $\Delta G_2^\circ$  and  $\Delta G_3^\circ$ . The failure of the simple TSA model for  $\Delta G_2^\circ$  and  $\Delta G_3^\circ$  appears to be due to a need to treat aromatic carbon and hydrogen atoms as distinct units. The results for  $\delta\Delta G_3^\circ$ , for example, suggest that the aromatic carbon is considerably more hydrophilic and the aromatic hydrogen considerably more hydrophobic than aliphatic methylene units on a per unit area basis.

The group surface area approach has the advantage of providing all group area terms in one calculation. It is not necessary to account directly for group proximity effects since these are included implicitly in the area calculation. Consequently it can be used to estimate  $\Delta G_1^\circ$ ,  $\Delta G_2^\circ$ , and  $\Delta G_3^\circ$  for compounds for which data are unavailable or difficult to obtain.

## Isopiestic Determination of the Osmotic Coefficients of Aqueous $\text{Na}_2\text{SO}_4$ , $\text{MgSO}_4$ , and $\text{Na}_2\text{SO}_4\text{-MgSO}_4$ at 25 °C

Joseph A. Rard\*<sup>†</sup> and Donald G. Miller

University of California, Lawrence Livermore National Laboratory, Livermore, California 94550

The osmotic coefficients of aqueous  $\text{Na}_2\text{SO}_4$ ,  $\text{MgSO}_4$ , and an equimolar mixture of these salts have been measured by the isopiestic method at 25 °C. The solubilities of KCl,  $\text{Na}_2\text{SO}_4 \cdot 10\text{H}_2\text{O}$ , and  $\text{MgSO}_4 \cdot 7\text{H}_2\text{O}$  have also been determined. The results are compared to other available activity and solubility data for these salts. Least-squares equations were used to represent these data and to calculate activity coefficients of  $\text{Na}_2\text{SO}_4$  and  $\text{MgSO}_4$ . Discrepancies between isopiestic and freezing-point-depression measurements for most 2-2 electrolytes may be due to the neglect of the temperature dependence of the heat capacities.

### Introduction

Solutions of  $\text{Na}_2\text{SO}_4$  and  $\text{MgSO}_4$  are of geochemical interest because of their presence in seawater and certain other natural brines. In addition,  $\text{Na}_2\text{SO}_4$ ,  $\text{Na}_2\text{SO}_4 \cdot 10\text{H}_2\text{O}$ ,  $\text{MgSO}_4$ ,  $\text{MgSO}_4 \cdot 7\text{H}_2\text{O}$ ,  $\text{Na}_2\text{SO}_4 \cdot \text{MgSO}_4 \cdot 4\text{H}_2\text{O}$ , and  $\text{Na}_2\text{SO}_4 \cdot \text{MgSO}_4 \cdot 2.5\text{H}_2\text{O}$  all form natural minerals, so data for their solutions are of interest in interpreting their dissolution behavior.

The mutual diffusion coefficients of aqueous  $\text{Na}_2\text{SO}_4$  and  $\text{MgSO}_4$  have recently been reported (1). To convert these values to thermodynamic diffusion coefficients requires activity-coefficient or osmotic-coefficient derivatives. Examination of the available activity data for these salts at 25 °C indicated discrepancies of up to several percent between the various studies. In addition, osmotic coefficients from the freezing-point-depression and isopiestic methods are not in very good

### Literature Cited

- (1) R. B. Hermann, *J. Phys. Chem.*, **76**, 2754 (1972).
- (2) G. L. Amidon, S. H. Yalkowsky, and S. Leung, *J. Pharm. Sci.*, **63**, 1858 (1974).
- (3) G. L. Amidon, S. H. Yalkowsky, S. T. Anik, and S. C. Valvani, *J. Phys. Chem.*, **79**, 2239 (1975).
- (4) G. L. Amidon and S. T. Anik, *J. Phys. Chem.*, **64**, 970 (1960).
- (5) S. H. Yalkowsky, G. L. Flynn, and T. G. Slunick, *J. Pharm. Sci.*, **61**, 853 (1972).
- (6) C. Tsouopoulos and J. M. Prausnitz, *Ind. Eng. Chem. Fundam.*, **10**, 593 (1971).
- (7) D. R. Stull, E. F. Westrum, and G. L. Sinke, "The Chemical Thermodynamics of Organic Compounds", Wiley, New York, 1969.
- (8) S. T. Anik, Ph.D. Thesis, University of Wisconsin, Madison, WI, 1978.
- (9) Z. Yoshida and E. Osawa, *J. Am. Chem. Soc.*, **67**, 1487 (1965).
- (10) G. L. Amidon, R. S. Pearman, and S. T. Anik, *J. Theor. Biol.*, **77**, 161 (1979).

Received for review March 24, 1980. Accepted August 25, 1980. This work was supported by grants from the Upjohn Company, the University of Wisconsin Graduate School, and the Public Health Service (GM-20437).

**Supplementary Material Available:** Solubility and free energy of solution (aqueous), heats of fusion, melting points, and vapor pressures of alkyl aromatic compounds (15 pages). Ordering information is given on any current masthead page.

agreement for  $\text{MgSO}_4$  (2, 3). Since differentiation yields even larger uncertainties, it was clear that additional accurate activity measurements are required for these salts. In this report isopiestic data are presented for aqueous  $\text{Na}_2\text{SO}_4$ ,  $\text{MgSO}_4$ , and their equimolar mixture.

### Experimental Section

The isopiestic apparatus is the same as previously described (4). The measurements were performed at  $25.00 \pm 0.005$  °C (IPTS-68). The molecular weights used were 18.0154 g/mol for  $\text{H}_2\text{O}$ , 142.037 g/mol for  $\text{Na}_2\text{SO}_4$ , 120.363 g/mol for  $\text{MgSO}_4$ , 95.211 g/mol for  $\text{MgCl}_2$ , 74.551 g/mol for KCl, and 98.074 g/mol for  $\text{H}_2\text{SO}_4$ .

The preparation and analyses of the KCl and  $\text{H}_2\text{SO}_4$  isopiestic standards have been described elsewhere (4, 5). The  $\text{Na}_2\text{SO}_4$  and  $\text{MgSO}_4$  were from the same high-purity samples used for the diffusion coefficient study (1). Mallinckrodt analytical reagent  $\text{MgSO}_4$  and Baker Analyzed  $\text{Na}_2\text{SO}_4$  were recrystallized and filtered. A sample of the  $\text{MgSO}_4$  stock solution was evaporated to dryness and then analyzed for impurities by using direct current arc optical emission spectroscopy. The impurities found were ca. 0.003% Ca, 0.001% B, 0.0008% Si, and less than 0.00002% Na by weight. Other alkali and alkaline earths were below their detection limits. The stock solutions' concentrations were obtained with a precision of  $\sim 0.01\%$  by dehydration of weighed samples at 500 °C.

The isopiestic molalities are the average of two samples, and are known to at least  $\pm 0.1\%$  (in most cases to  $\pm 0.05\%$  or better). All weights were converted to mass. The molalities of the solutions at isopiestic equilibrium are listed in Tables I and II. Also included in Table II are four  $\text{MgCl}_2$  points; up to 8 weeks were allowed for these low-concentration equilibrations. The osmotic coefficients of the KCl and  $\text{H}_2\text{SO}_4$  isopiestic standards were calculated from available equations (6, 7). The

<sup>†</sup> Visiting Assistant Professor of Geology 1977-8, University of Illinois at Urbana-Champaign, tenure served as participating guest at Lawrence Livermore Laboratory. Direct correspondence to this author at Lawrence Livermore Laboratory.